Ultra-wide band signal generation using a coupling-tunable silicon microring resonator

Yunhong Ding, Bo Huang, Christophe Peucheret, Jing Xu, Haiyan Ou, Xinliang Zhang, Dexiu Huang

Ultra-wide band signal generation using a coupling-tunable silicon microring resonator

Yunhong Ding,[1,*] Bo Huang,[1,3] Christophe Peucheret,[1,2] Jing Xu,[1] Haiyan Ou,[1] Xinliang Zhang,[3] and Dexiu Huang[3]

[1]*Department of Photonics Engineering, Technical University of Denmark, 2800 Kgs. Lyngby, Denmark*

[2]*University of Rennes 1 - ENSSAT, FOTON Laboratory - CNRS UMR 6082, 22300 Lannion, France*

[3]*Wuhan National Laboratory for Optoelectronics, School of Optoelectronics Science and Engineering, Huazhong University of Science and Technology, Wuhan, 430074, Hubei, China*

[*]*yudin@fotonik.dtu.dk*

Abstract: Ultra-wide band signal generation using a silicon microring resonator tuned to an NRZ-DPSK modulated optical carrier is proposed and demonstrated. The scheme is shown to enable the generation of UWB signals with switchable polarity and tunable bandwidth by simply tuning the coupling regions of the microring resonator. Monocycle pulses with both negative and positive polarities are successfully synthesized experimentally.

OCIS codes: (060.5625) Radio frequency photonics; (230.3120) Integrated optics devices; (350.4010) Microwaves.

References and links

1. F. Zeng and J. Yao, "An approach to ultrawideband pulse generation and distribution over optical fiber," IEEE Photon. Technol. Lett. **18**, 823–825 (2006).
2. J. Yao, F. Zeng, and Q. Wang, "Photonic generation of ultrawideband signals," J. Lightwave Technol. **25**, 3219–3235 (2007).
3. J. Dong, X. Zhang, J. Xu, and D. Huang, "Ultrawideband monocycle generation using cross-phase modulation in a semiconductor optical amplifier," Opt. Lett. **32**, 1223–1225 (2007).
4. Q. Wang and J. Yao, "Switchable optical UWB monocycle and doublet generation using a reconfigurable photonic microwave delay-line filter," Opt. Express **15**, 14667–14672 (2007).
5. E. Zhou, X. Xu, K. S. Lui, and K. K. Y. Wong, "A power-efficient ultra-wideband pulse generator based on multiple PM-IM conversions," IEEE Photon. Technol. Lett. **22**, 1063–1065 (2010).
6. Y. Yue, H. Huang, L. Zhang, J. Wang, J. Yang, O. Yilmaz, J. Levy, M. Lipson, and A. Willner, "UWB monocycle pulse generation using two-photon absorption in a silicon waveguide," Opt. Lett. **37**, 551–553 (2012).
7. S. Pan and J. Yao, "Switchable UWB pulse generation using a phase modulator and a reconfigurable asymmetric Mach–Zehnder interferometer," Opt. Lett. **34**, 160–162 (2009).
8. F. Liu, T. Wang, Z. Zhang, M. Qiu, and Y. Su, "On-chip photonic generation of ultra-wideband monocycle pulses," Electron. Lett. **45**, 1247 (2009).
9. D. Marpaung, L. Chevalier, M. Burla, and C. Roeloffzen, "Impulse radio ultrawideband pulse shaper based on a programmable photonic chip frequency discriminator," Opt. Express **19**, 24838–24848 (2011).
10. Y. Zhang, X. Zhang, F. Zhang, J. Wu, G. Wang, and P. P. Shum, "Photonic generation of millimeter-wave ultra-wideband signal using microfiber ring resonator," Opt. Commun. **284**, 1803–1806 (2011).
11. B. Luo, J. Dong, Y. Yu, and X. Zhang, "Bandwidth-tunable single-carrier UWB monocycle generation using a nonlinear optical loop mirror," IEEE Photon. Technol. Lett. **24**, 1646–1649 (2012).
12. Fed. Commun. Commission, Revision of Part 15 of the Commissions Rules Regarding Ultra-Wideband Transmission Systems, Tech. Rep. ET-Docket 98-153, FCC02-48, 2002.
13. Y. Ding, M. Pu, L. Liu, J. Xu, C. Peucheret, X. Zhang, D. Huang, and H. Ou, "Bandwidth and wavelength-tunable optical bandpass filter based on silicon microring-MZI structure," Opt. Express **19**, 6462–6470 (2011).

#205564 - $15.00 USD Received 27 Jan 2014; revised 24 Feb 2014; accepted 25 Feb 2014; published 6 Mar 2014

14. M. Bolea, J. Mora, B. Ortega, and J. Capmany, "Optical UWB pulse generator using an N tap microwave photonic filter and phase inversion adaptable to different pulse modulation formats," Opt. Express **17**, 5023–5032 (2009).
15. M. Aamer, D. J. Thomson, A. M. Gutiérrez, A. Brimont, F. Y. Gardes, G. T. Reed, J. M. Fedeli, A. Hakansson, and P. Sanchis, "10 Gbit/s error-free DPSK modulation using a pushpull dual-drive silicon modulator," Opt. Commun. **304**, 107–110 (2013).
16. L. Vivien, J. Osmond, J.-M. Fédéli, D. Marris-Morini, P. Crozat, J.-F. Damlencourt, E. Cassan, Y. Lecunff, and S. Laval, "42 GHz p.i.n Germanium photodetector integrated in a silicon-on-insulator waveguide," Opt. Express **17**, 6252–6257 (2009).
17. Q. Wang and J. Yao, "Switchable optical UWB monocycle and doublet generation using a reconfigurable photonic microwave delay-line filter," Opt. Express **15**, 14667–14672 (2007).

1. Introduction

Ultra-wide band (UWB) over fiber is a promising technique to overcome the inherent limited propagation range of traditional electrical UWB signals in high data rate wireless applications [1]. As a consequence, the photonic generation of UWB signals has been a very active area of research over the past few years, and numerous techniques have been suggested and demonstrated [2–6]. One of the principles underlying a number of those techniques is to perform phase modulation of an optical carrier with Gaussian pulses, followed by phase-to-intensity modulation (PM-to-IM) conversion using a frequency discriminator or a dispersive element [2, 3]. PM-to-IM conversion can be achieved using the slopes of the transfer functions of optical filters, and the use of a Mach-Zehnder interferometer (MZI) [7], a silicon microring resonator (MRR) [8,9], and a microfibre ring resonator [10] have enabled the synthesis of UWB waveforms with adjustable polarity. However, the previously quoted methods rely on the generation of Gaussian electrical pulses, which may not be available from conventional electronic circuits. Recently, the use of a nonlinear optical loop mirror [11] and two-photon absorption in a silicon waveguide [6] have been demonstrated, showing the ability to synthesize UWB signals with tunable bandwidth.

In this paper, we propose to use phase modulation with standard non return-to-zero (NRZ) electronics in a Mach-Zehnder modulator (MZM) and to exploit the simultaneous phase shifts and intensity dips of an NRZ differential phase-shift keying (NRZ-DPSK) signal to generate an UWB signal after filtering by a silicon add-drop MRR whose resonance is tuned to the center frequency of the signal. We emphasise that this method is different from previously demonstrated techniques making use of Gaussian phase modulation followed by frequency discrimination such as in [8,9]. We show that, by proper adjustment of the coupling coefficients of the MRR, monocycle pulses with both negative and positive polarities can be obtained. Furthermore, the bandwidth of the UWB signal can be easily tuned by tuning the coupling coefficients of the MRR. We demonstrate the concept experimentally using a specially designed and fabricated silicon MRR.

2. Principle of the method

The principle of the method is depicted schematically in Fig. 1. A continuous wave (CW) laser is modulated in the NRZ-DPSK format in an MZM. The modulation results in intensity dips each time the phase of the signal is flipped between 0 and π. The modulated signal is then input to a silicon microring resonator in add-drop configuration (therefore with two coupling regions). In the proposed method, the CW laser needs to be tuned to a resonance frequency of the MRR. The output of the through port of the MRR is finally detected in a photodiode (PD). When the carrier wavelength of the NRZ-DPSK signal is tuned to a resonance, the MRR through output field E_t can be expressed in the time domain as

$$E_t(t+T) = ar_1r_2E_t(t) + [r_1E_{in}(t+T) - ar_2E_{in}(t)] \quad (1)$$

#205564 - $15.00 USD Received 27 Jan 2014; revised 24 Feb 2014; accepted 25 Feb 2014; published 6 Mar 2014

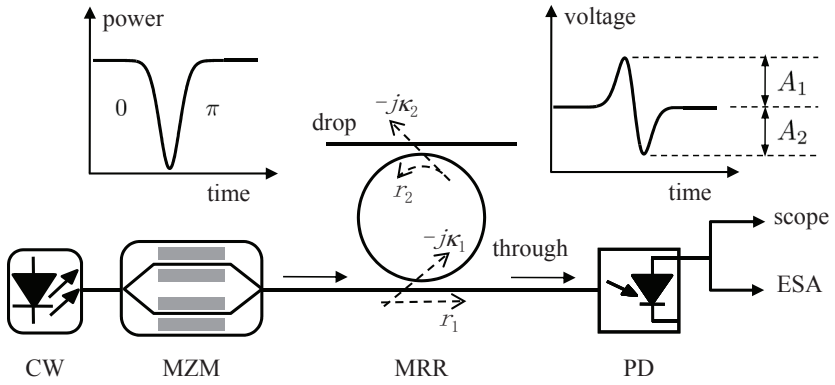

Fig. 1. Principle of the UWB generation method. The insets show typical simulated waveforms for the intensity of the NRZ-DPSK signal and the generated UWB signal.

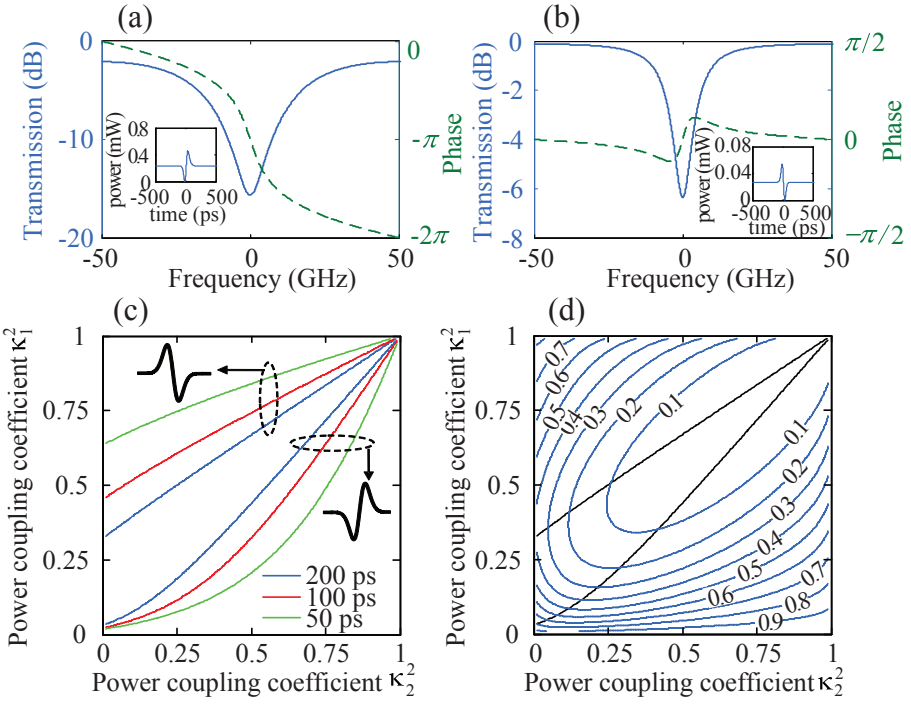

Fig. 2. Through transmission and phase response of an MRR with (a) $\kappa_1^2 = 0.824, \kappa_2^2 = 0.655$ and (b) $\kappa_1^2 = 0.18, \kappa_2^2 = 0.346$ and $a = 0.93$. The corresponding monocycle pulses with negative and positive polarity obtained with an electrical rise time of 100 ps are shown as insets in each case. (c) Calculated values of the MRR through and drop power coupling coefficients κ_1^2 and κ_2^2 resulting in monocycle pulses fulfilling the condition $A_1 = A_2$ (defined in Fig. 1) for three electrical driving signal rise times of 50 ps, 100 ps and 200 ps, respectively. (d) Normalized peak-to-peak power as a function of the MRR through and drop power coupling coefficients κ_1^2 and κ_2^2 for an electrical driving signal rise time of 200 ps, together with the combinations of κ_1^2 and κ_2^2 equalizing A_1 and A_2.

#205564 - $15.00 USD Received 27 Jan 2014; revised 24 Feb 2014; accepted 25 Feb 2014; published 6 Mar 2014

where $E_{in}(t)$ is the electric field of the input NRZ-DPSK signal and a and T are the field roundtrip transmission coefficient and roundtrip time of the MRR, respectively. r_1 and r_2 are the field transmission coefficients of the through and drop coupling regions, respectively, with the corresponding field coupling coefficients κ_1 and κ_2 satisfying $r_1^2+\kappa_1^2=1$ and $r_2^2+\kappa_2^2=1$ for lossless coupling. According to Eq. (1), it can be found that an overshoot followed by a dip, or a dip followed by an overshoot can be obtained each time an intensity dip of the NRZ-DPSK signal is input to the MRR if $r_1 < ar_2$ or $r_1 > ar_2$, respectively. In addition, by adjusting the coupling coefficients κ_1 and κ_2 at the through and drop couplers of the resonator, respectively, the amplitudes of the overshoots and dips with respect to the average signal level (A_1 and A_2, respectively, as defined in Fig. 1) can be equalized, resulting in a typical monocycle pulse shape as simulated in Figs. 2(a) and 2(b). The values of the optimum coupling coefficients depend on the fall and rise times of the intensity dips of the NRZ-DPSK modulated signal, and therefore on the electrical driving signal rise time and modulator bandwidth. This point is illustrated in Fig. 2(c), which represents the combination of values of κ_1^2 and κ_2^2 for which $A_1=A_2$ for three signal rise times of 50 ps, 100 ps and 200 ps, respectively. It can be seen that, for each value of the rise time of the phase modulating signal, two sets of (κ_1^2,κ_2^2) parameters that equalize A_1 and A_2 can be found. Each set corresponds to a given polarity of the monocycle pulse, as illustrated in Fig. 2(c). Consequently, optimization of the UWB waveform requires MRRs with tunable coupling coefficients. To obtain a monocycle with higher radio frequency (RF) power, a higher peak-to-peak power (A_1+A_2) is preferred. Figure 2(d) shows the normalized peak-to-peak power as a function of the MRR through and drop power coupling coefficients κ_1^2 and κ_2^2 in case the rise time of the electrical driving signal is 200 ps. The combinations of κ_1^2 and κ_2^2 equalizing A_1 and A_2 for this rise time are also reproduced for reference with black curves. One can find that, as κ_2^2 decreases, a higher peak-to-peak amplitude will be obtained for the generated monocycle pulses.

Figure 3 analyzes how the 10 dB bandwidth and peak frequency of the generated UWB spectra evolve as a function of power coupling coefficient κ_2^2 for both positive and negative polarities of the monocycle pulse and for different electrical signal rise time values. One can find that, as κ_2^2 increases, both the 10 dB bandwidth and peak frequency increase for both generated positive and negative polarity UWB signals, as shown in Figs. 3(a) and 3(b). This

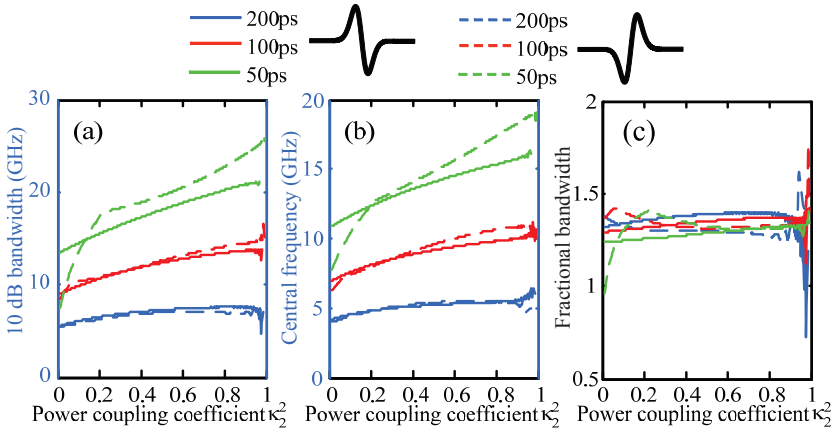

Fig. 3. Calculated (a) 10 dB bandwidth, (b) peak frequency, and (c) fractional bandwidth of both positive and negative polarity UWB signal spectra as a function of power coupling coefficient κ_2^2 for electrical driving signal rise times of 50 ps, 100 ps and 200 ps. κ_1^2 is selected to equalize A_1 and A_2 for all generated UWB signals.

#205564 - $15.00 USD Received 27 Jan 2014; revised 24 Feb 2014; accepted 25 Feb 2014; published 6 Mar 2014

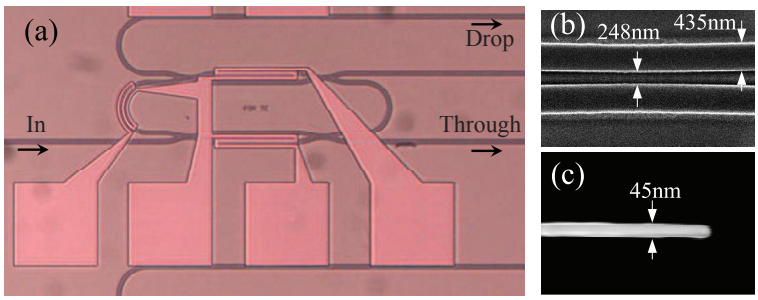

Fig. 4. (a) Microscope picture of the fabricated device. Scanning electron microscope (SEM) pictures of (b) one of the coupling regions and (c) the tip of the silicon nano-taper.

is because, as κ_2^2 increases, the Q value of the MRR decreases, leading to a shorter photon lifetime and consequently shorter overshoot of the generated UWB signal and larger 10 dB bandwidth. The tunable ranges of both 10 dB bandwidth and peak frequency increase as the electrical driving signal rise time decreases. For different electrical driving signal rise times, both positive and negative polarity UWB signals exhibit a high fractional bandwidth around 130%, as shown in Fig. 3(c), which meets the Federal Communications Commission (FCC) requirement of 20% [12].

3. Fabricated device

In order to test this new concept, a silicon MRR with adjustable through and drop power coupling coefficients was designed and fabricated. The tunability of the coupling coefficients is achieved by two MZI structures which act as through and drop couplers. Thermal tuning enables to control the relative phase shifts between the two arms of each MZI, and consequently the power coupling ratio between the ring and the input and drop waveguides. The device was fabricated on a silicon-on-insulator (SOI) wafer with top silicon thickness of 250 nm and buried silicon oxide of 3 μm. The fabrication process is identical to the one described in details in [13]. Figure 4(a) shows a picture of the fabricated device. The waveguides are 435 nm wide and covered with 600 nm benzocyclobutene (BCB) as top cladding layer. A coupling gap of 248 nm is introduced in each coupling region of the MZIs, as shown in Fig. 4(b). Three heaters (100 nm thick titanium with 5 nm thick gold) are deposited on top of part of the ring waveguide and of one of the arms in each of the MZI structures in order to perform thermal tuning of the resonance wavelength and the MRR coupling coefficients. The device operates in the transverse magnetic (TM) mode and has a free-spectral range (FSR) of 100 GHz. The input and output silicon waveguides are inversely tapered to 45 nm, as shown in Fig. 4(c), and covered by a polymer (SU8 2005) waveguide to form a nano-coupler to improve the coupling loss to tapered fibres. The insertion loss is measured to be 10.5 dB for the TM mode before heating the two coupling regions. The high insertion loss is potentially due to optical power leakage to the metal heater above the waveguide. It could be improved by increasing the thickness of the BCB layer.

4. Experimental demonstration

The fabricated device was used in an UWB generation experiment at 1.25 Gbit/s. The experimental set-up is shown in Fig. 5. The electrical signals driving an MZM biased at a transmission minimum in push-pull mode were generated at 1.25 Gbit/s by programming a 40 Gbit/s bit pattern generator, hence resulting in fast rise and fall times. Low pass filtering of the driving signals with a 4th order Bessel filter having a 7.5 GHz cut-off frequency was performed in order to in-

#205564 - $15.00 USD Received 27 Jan 2014; revised 24 Feb 2014; accepted 25 Feb 2014; published 6 Mar 2014

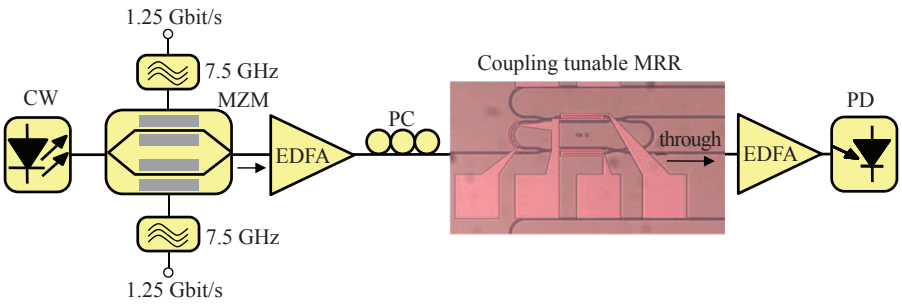

Fig. 5. Experimental setup.

crease their rise time to ∼50 ps. It should be pointed out that this filtering is required by the fast rise time of the electronics available in our laboratory. In practice the proposed method will directly accommodate the rise times of lower speed signal generation electronics compatible with UWB applications. Similarly, the choice of the 1.25 GHz frequency is a consequence of available equipment but the concept is straightforward to implement at lower repetition rates. The optical signal was amplified by an erbium-doped fiber amplifier (EDFA). Afterwards, its state-of-polarization was aligned to the TM mode by a polarization controller (PC) and input to the chip with an input power of about 18 dBm. The output signals from the MRR were amplified by another EDFA and detected with a high-speed photodiode with cut-off frequency of 45 GHz. Figure 6 shows the experimental results for the generation of UWB signals with both negative and positive polarities. The CW laser was precisely tuned to a resonance of the MRR, as shown in the optical spectra of Figs. 6(a) and 6(d). The power coupling coefficients of the through and drop couplers of the MRR were thermally tuned to obtain the balanced monocycle pulses of Figs. 6(b) and 6(e). Figures 6(c) and 6(f) show the radio-frequency spectra of the UWB signal after photodetection for generated UWB signals of negative and positive polarities, respectively. The MRR insertion loss increases when the polarity is tuned from negative to positive, as shown in Figs. 6(a) and 6(d). This is due to the fact that higher coupling coefficients are used in order to balance the generated monocycle pulses, which further results in narrower UWB pulses (see Fig. 6(e)) and broader RF spectra (see Fig. 6(f)). The independent settings of κ_1 and κ_2 offer a large degree of flexibility to tune the UWB waveform and the resulting radio-frequency spectrum.

5. Discussion

Due to the short electrical rise time of the driving signals used in our experimental demonstration, the measured RF spectra shown in Figs. 6(c) and 6(f) have broad bandwidths compared with the FCC mask. In order to map the FCC mask, a microwave filter could be used to tailor the RF spectrum [17]. Otherwise, a slower rise time is needed and more complex pulse shapes would be required [14]. Figure 6 shows a simulated typical UWB monocycle pulse (detailed in Fig. 7(a)) generated by our proposed MRR method and the corresponding RF spectrum (see Fig. 7(b)) with $\kappa_1^2 = 0.462$, $\kappa_2^2 = 0.015$ and rise time of 100 ps. A Gaussian monocycle pulse obtained by first order differentiation of a Gaussian pulse and having the same time delay between the peak and dip as the MRR-generated monocycle, as well as its calculated RF spectrum, are also shown for comparison. The RF spectrum of the MRR-generated UWB monocycle pulse appears to be more compliant with the FCC mask than that of the Gaussian monocycle. Once such a monocycle pulse has been synthesized, more complex pulse shapes could be obtained by cascading additional MRRs, as demonstrated in [9].

#205564 - $15.00 USD Received 27 Jan 2014; revised 24 Feb 2014; accepted 25 Feb 2014; published 6 Mar 2014

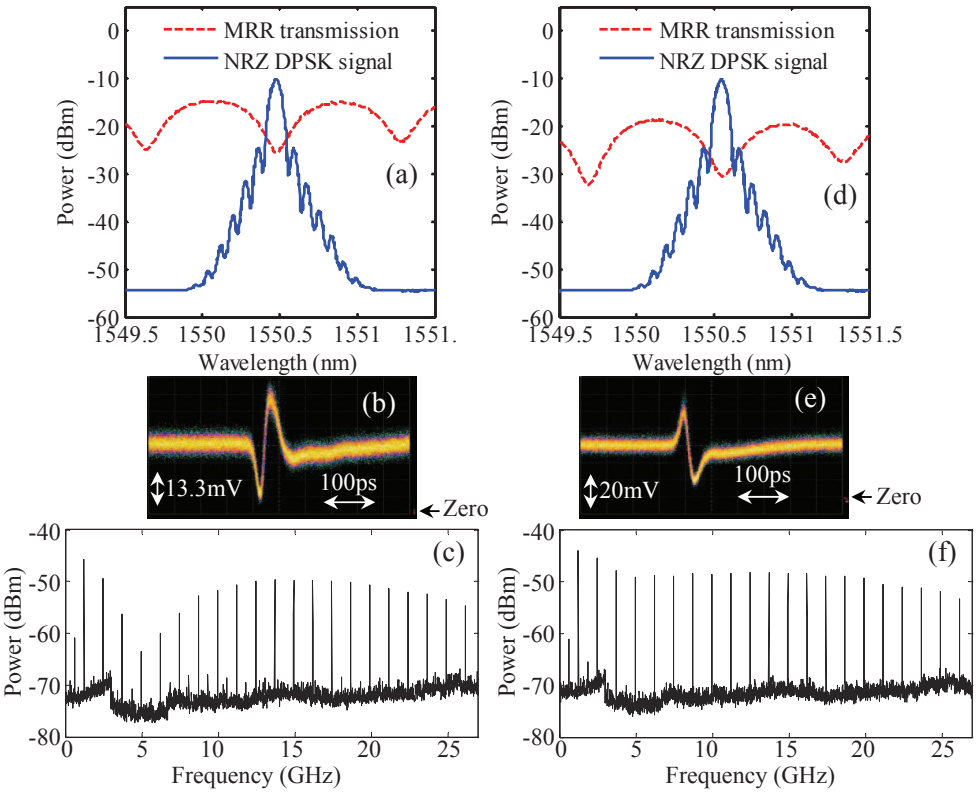

Fig. 6. Measured transfer function of the through transmission of the MRR, together with the spectrum of the optical NRZ-DPSK signal at 1.25 Gbit/s for generations of (a) negative and (d) positive polarity monocycle signals. Waveform of the generated (b) negative and (e) positive polarity UWB monocycle pulse at 1.25 Gbit/s, and (c) and (f) corresponding radio frequency spectra obtained from a 1.25 GHz periodic pulse train.

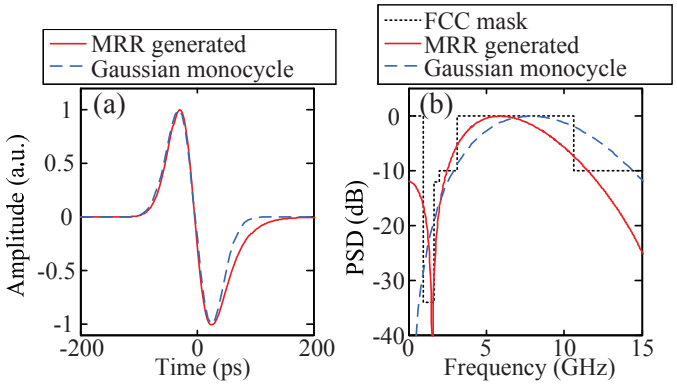

Fig. 7. (a) Simulated UWB monocycle pulse generated by the proposed MRR with $\kappa_1^2 = 0.462$, $\kappa_2^2 = 0.015$ and rise time of 100 ps, as well as matching Gaussian monocycle pulse obtained by first order differentiation of a Gaussian pulse. (b) Corresponding RF spectra. The FCC mask is also plotted for comparison.

#205564 - $15.00 USD Received 27 Jan 2014; revised 24 Feb 2014; accepted 25 Feb 2014; published 6 Mar 2014

Using the proposed technique, a compact UWB signal generator could potentially be realised by monolithically integrating the coupling-tunable silicon MRR with a silicon MZM [15] and germanium detectors [16] on a single chip.

6. Conclusion

A novel method to generate an UWB signal using a silicon MRR and a phase modulated signal generated using conventional NRZ electronics in a Mach-Zehnder modulator has been proposed and demonstrated. It has been shown that proper adjustment of the coupling coefficients of the add-drop MRR enables the synthesis of high-quality monocycle pulses with tunable bandwidth. A stable and compact silicon-on-insulator MRR with 100 GHz FSR and tunable coupling coefficients has been specially designed and fabricated for this application. The fabricated device was applied to the generation of an UWB signal at 1.25 Gbit/s with both negative and positive polarities.

Acknowledgments

This work was partly supported by the Danish Council for Independent Research (project 1337-00152).

#205564 - $15.00 USD Received 27 Jan 2014; revised 24 Feb 2014; accepted 25 Feb 2014; published 6 Mar 2014